Effects of Roughness and Coating on Frictional Behavior of Planetary Gear Type Torque-Sensing LSD*1

J. ANDO H. ANDO H. SAITO H. TAKUNO T. HARA N. SAKAI
Y. YAMASHITA M. TOHYAMA T. OHMORI

A planetary gear type torque-sensing limited slip differential (LSD) must prevent stick slip and allow smooth sliding between contact surfaces. This development aimed to achieve a fine roughness on the sliding surfaces along the planetary gear circumference to make it possible to acquire stable frictional characteristics.

Furthermore, these frictional characteristics can be studied in theory without testing on actual units by mixed lubrication analysis, which models the roughness of the planetary gear circumference. In addition, applying carbon-based hard-coating to the planetary gear secured durability against wear and seizure, characteristics normally sacrificed at the expense of roughness.

***Key Words**: power transmission, all-wheel drive system, limited slip differential, roughness, coating*

1. Introduction

In recent years, the market has been demanding an even higher standard of safety and dynamic stability and as such people worldwide are again recognizing the importance of all-wheel drive (AWD).

Various AWD mechanisms have been developed to respond to diversifying vehicle specifications. AWD systems can be broadly divided into the full-time, the on-demand and the part-time systems, as shown in **Fig. 1**. AWD development became more active around the early 1980s, with several systems being developed since, each with their unique advantages.

Figure 2 is an example of a full-time system, showing a mechanical differential structure that is used as a center differential. This AWD system incorporates a planetary gear type torque-sensing limited slip differential (LSD) and is adopted widely in high performance vehicles. This system constantly transmits engine torque to all four wheels, enabling stable transmission of driving force. The system is also highly responsive and reliable as its full-time function is achieved by a differential mechanism that allows the front and rear wheels to rotate at different speeds and because of the mechanical structure of the system[1), 2)].

This report describes the tribological technology that makes a significant contribution to the reliability of the planetary gear type torque-sensing LSD.

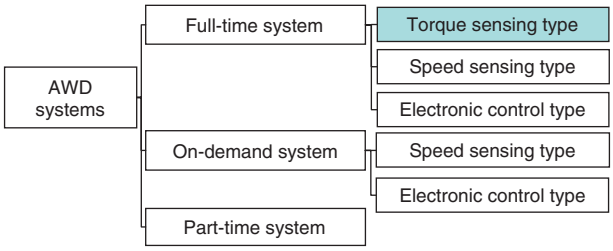

Fig. 1 Classification of AWD systems

2. Structure of Planetary Gear Type Torque-Sensing LSD

The planetary gear type torque-sensing LSD has a differential limiting function as well as a normal differential function. This report describes this specialized AWD system. This AWD-specific gear type torque-sensing LSD has a mechanism that obtains the differential limiting force depending on the engine input. As shown in **Fig. 2**, it consists of planetary gears, a housing, a sun gear, an internal gear, and washers. Its distinctive feature is the way that the planetary gears are retained in the housing. The planetary gear can be housed so it can rotate without a securement pin inside the bore provided in the housing. The planetary gear top land receives normal vector load from the housing bore surface. The engine torque input to the housing is distributed to the sun gear and the internal gear through the planetary gears. The differential limiting function mainly utilizes the friction forces of the washer

**1 This paper was prepared based on a report from the Society of Automotive Engineers of Japan. (Vol. 42, No. 2, March 2011, p. 379-384).*

surfaces and the planetary gear circumference shown in **Fig. 3**. Torque distribution to the sun gear and the internal gear is structurally unequal in proportion to each meshing radius. **Figure 4** shows one example of an AWD layout with planetary gear type torque-sensing LSD. Because of the unequal torque distribution, this planetary gear type torque-sensing LSD is designed specifically for application with center differentials [2].

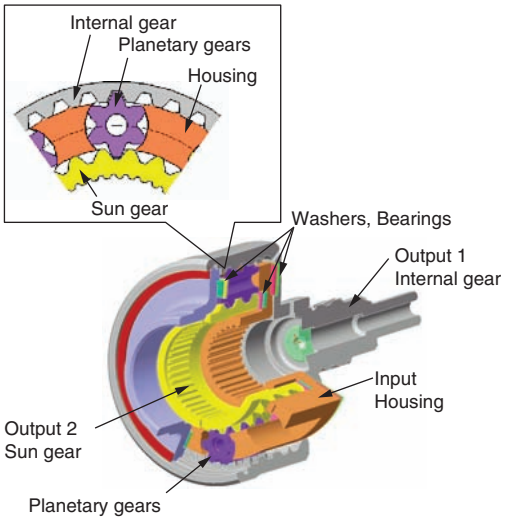

Fig. 2 Structure of planetary gear type torque-sensing LSD

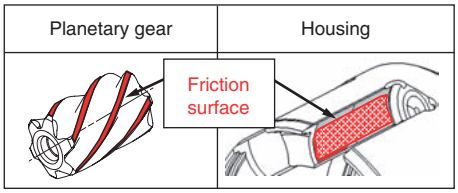

Fig. 3 Sliding surfaces of the planetary gear circumference and housing bore

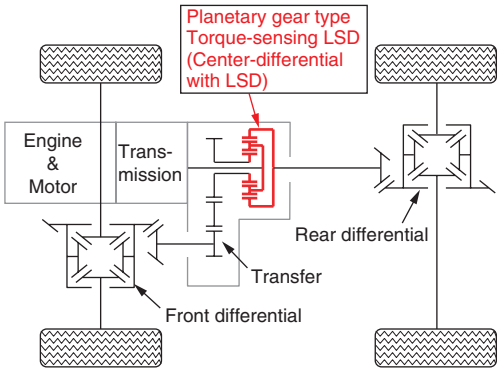

Fig. 4 AWD layout of planetary gear type torque-sensing LSD

3. Tribology of Planetary Gear Type Torque-Sensing LSD

3. 1. Analysis of Frictional Behavior and Friction Surface Profile of Planetary Gear Type Torque-Sensing LSD

Depending on the driving conditions of the vehicle, different rotation may occur on planetary gear type torque-sensing LSDs while internal friction is generated. In such cases, the friction must be generated smoothly while suppressing stick-slip at the friction surface. Stick-slip is known to occur when the dependence of the friction coefficient (μ) on velocity (v) (i.e., the μ-v characteristic) has a negative slope [3]. Therefore, an effective countermeasure to prevent stick-slip is to reduce the effect of the negatively-sloped μ-v characteristic and bring it closer to a positive slope ($d\mu/dv \geqq 0$). The μ-v characteristic can be greatly affected by optimizing the friction surface profiles and materials, and the various types of additives compounded in the fluid [4), 5)]. Improving the μ-v characteristic is extremely important for enhancing vehicle quietness.

Figure 5 shows the relationship between vibration and the μ-v slope in vehicle types A and B. The vibration sensitivity of vehicle B differs from vehicle A because the quietness and the anti-vibration performance of the vehicles themselves differ. This means that the anti-vibration performance (μ-v characteristic) required for the LSD differs between vehicle types. In other words, vehicle B requires an LSD with superior anti-vibration performance compared to vehicle A.

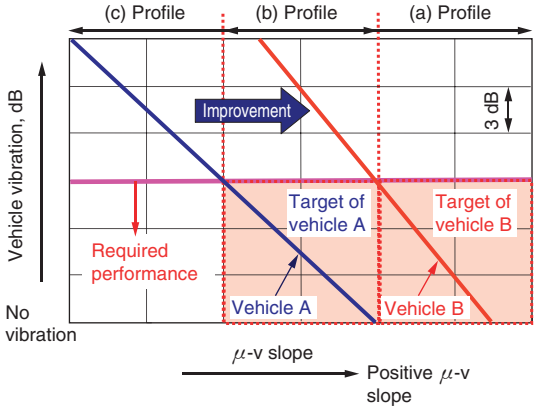

Fig. 5 Relationship between vehicle vibration amount and μ-v slope (Vehicle A vs B)

Figures 6 (a), (b), (c) and **7** show friction surface profiles of three types of planetary gear circumference and the housing bore face respectively as examples of vibration control technology (specifically, the suppression of self-excited vibration) applied to help resolve this issue. The friction surface roughnesses were set to *Ra*=2.5, 1.25, and 0.125 μm for the planetary gear surfaces, and *Ra*=0.6 μm for the housing bore surface. Surface roughnesses were measured with a stylus roughness measuring apparatus in accordance with JIS B 0601-2001 (ISO 4287-1997) and with measurement length of 4 mm and a cut-off of 0.8 mm as conditions. With respect to the anti-vibration effect of these concave-convex profiles, we attempted to interpret the relationship between the friction surface roughness and the μ-v characteristic using lubrication models of the planetary gear circumference and the housing bore face.

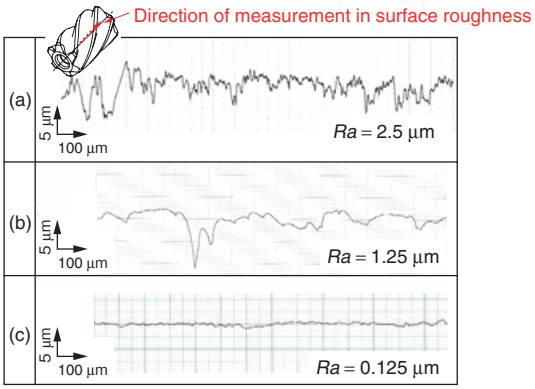

Fig. 6 Sliding surface profile of the planetary gear circumference
(a) *Ra* = 2.5 μm, (b) *Ra* = 1.25 μm, (c) *Ra* = 0.125 μm

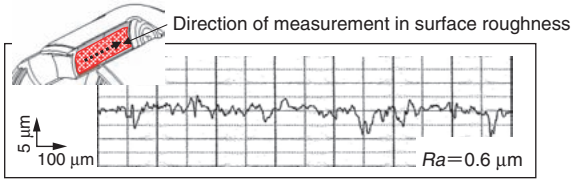

Fig. 7 Sliding surface profile of the housing bore

The friction of this sliding material in fluid is illustrated in **Fig. 8**. This figure assumes a mixed lubrication condition in which hydrodynamic friction due to fluid shear resistance coexists with boundary friction due to solid contact. This analysis also focused on analyzing friction characteristics in macroscopic lubrication conditions such as boundary and mixed lubrication, which vary in accordance to the oil film reaction forces of the friction surfaces. The analysis disregarded the effect of fluid additives, which decreases as the oil film thickness increases [6].

For theoretical analysis, **Fig. 9** is a simplified model of the two frictional surfaces, planetary gear circumference and the housing bore face.

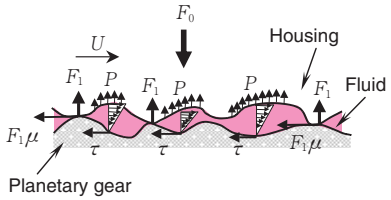

Fig. 8 Concept of friction force (in fluid)

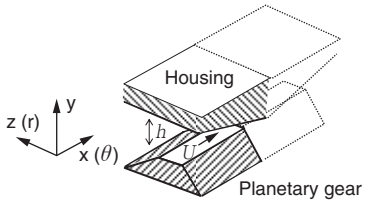

Fig. 9 Mixed lubrication model of sliding surface roughness

The housing bore face and the planetary gear circumference were assumed to have wedge-shaped projections with the height profiles shown in **Figs. 10**, **11**(a), (b), and (c), respectively. Furthermore, each height of the wedge-shaped projections was set to the average value of each roughness (*Ra*), and each pitch was the representative value of the roughness wavelength obtained by fast Fourier transform (FFT) analysis of each roughness.

The drag of the solid contacting portions F_1 caused by the pressing force F_0 of the housing input is expressed as follows.

$$F_1 = F_0 - \iint P \, dr \, d\theta \tag{1}$$

where, P is the hydraulic reaction force of the fluid, and r and θ indicate the directions vertical to the sliding and circumferential direction (sliding direction), respectively as shown in **Fig. 9**. The friction torque T_F caused by solid friction is expressed as follows.

$$T_F = \int \frac{2\pi r^2 F_1 \mu_b}{A} dr \tag{2}$$

where, A represents the apparent contact area of the friction surfaces, and μ_b represents the coefficient of boundary friction between solids.

Torque T_f by fluid viscosity is expressed as follows.

$$T_f = \iint \tau r \, dr d\theta \tag{3}$$

where, τ is the fluid shear stress working on the wall surfaces. As the following equations show, P is expressed by a simplified hydrodynamic motion equation and τ is expressed by a Newtonian viscosity equation.

$$h^3 \frac{\partial^2 P}{\partial x^2} + h^3 \frac{\partial^2 P}{\partial z^2} = 6MU \frac{dh}{dx} \quad (4)$$

$$\tau = \frac{h}{2} \frac{dP}{dx} + M \frac{U}{h} \quad (5)$$

where, M represents the fluid viscosity and U represents the sliding velocity.

Thus, the total torque T_0 is as follows.

$$T_0 = T_F + T_f \quad (6)$$

The total friction coefficient, which includes the boundary friction considering the hydraulic reaction force, and the hydrodynamic friction due to fluid shear resistance, can be calculated from T_0. The coefficient of boundary friction due to the solid friction was set to μ_b=0.12 and the pressing force F_0 was determined as 3 800 N, which was converted from the torque of an actual unit.

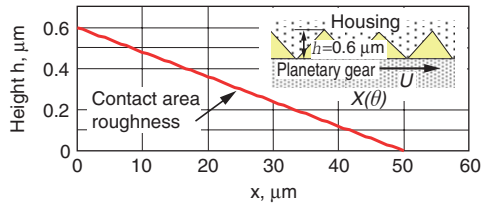

Fig. 10 Housing bore sliding surface model (x direction)

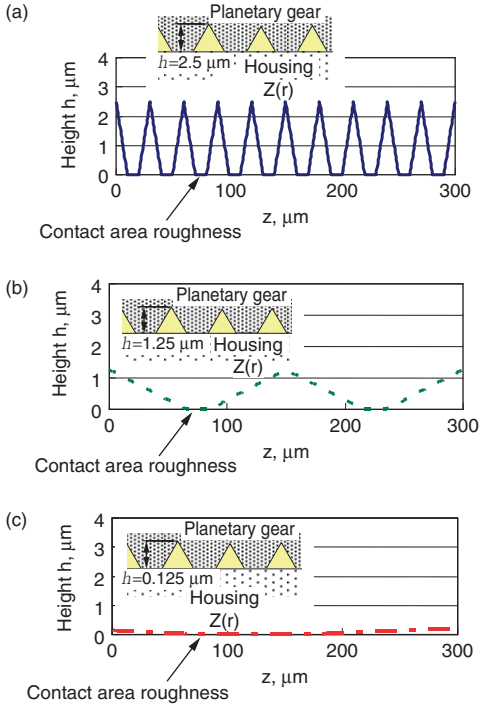

Fig. 11 Sliding surface model of the planetary gear circumference (z direction)
(a) Ra = 2.5 µm, (b) Ra = 1.25 µm,
(c) Ra = 0.125 µm

The mixed lubrication analysis described above was conducted using three models provided with each of the three types of roughness for the planetary gear circumference shown in **Fig. 11**.

Figure 12 shows the results of an analysis using the surface roughness of **Fig. 11**(a). **Figure 12** indicates that the total friction coefficient could be calculated as the sum of the hydrodynamic friction coefficient, and the boundary friction coefficient considering the hydraulic reaction force. **Figure 13** shows analysis results indicating the relationship between the total friction coefficient and the sliding velocity created by the roughnesses of each friction surface. It was found that adding the profile shown in **Fig. 6**(a) gave the μ-v characteristic between the planetary gear circumference and the housing bore a positive slope.

As stated above, the anti-vibration performance of driving force transmission devices is largely influenced by the μ-v characteristic. By forming the roughness shown in **Fig. 6**(a) on the planetary gear circumference, the surface concave-convex profile prevents the formation of an excessive oil film in accordance with the increase in sliding velocity. This profile satisfies the target range of vehicle B, which requires the higher anti-vibration performance shown in **Fig. 5**.

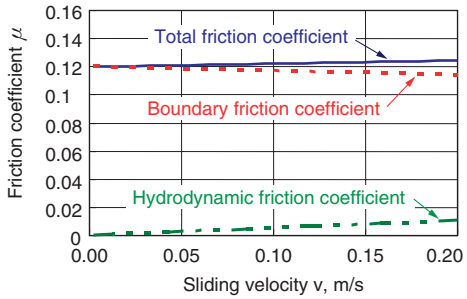

Fig. 12 Relationship between friction coefficient and sliding velocity (Calculated results: For roughness (a))

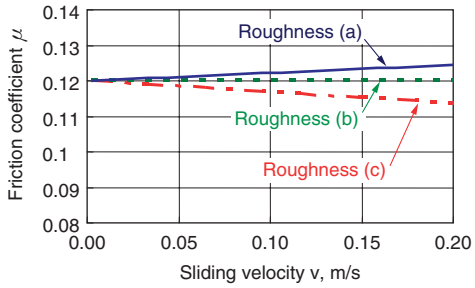

Fig. 13 Relationship between friction coefficient and sliding velocity (Calculated results: For roughness (a), (b), (c))

Although the moderate roughness profile displayed in **Fig. 6**(b) does not satisfy the required μ-v characteristic for vehicle B, it does satisfy that for vehicle A as shown in **Fig. 5**. In other words, some vehicles can achieve a sufficient anti-vibration effect with moderate roughness. In the case of the small roughness shown in **Fig. 6**(c), it is difficult to retain a positive μ-v slope, and does not satisfy the anti-vibration performance shown in **Fig. 5** even for vehicle A.

These surface concave-convex shapes enable a stable positively-sloped μ-v characteristic.

Moreover, **Fig. 14** shows the relationship between the μ-v characteristic and vehicle vibration for the actual unit (vehicle B). The μ-v slope indicated by the horizontal axis was obtained by dividing the friction coefficient at 0.186 m/s by the friction coefficient at 0.0046 m/s. The concave-convex profile of the planetary gear creates a positive μ-v slope, hence improving quietness of the vehicle. This result coincides with theoretical experiments.

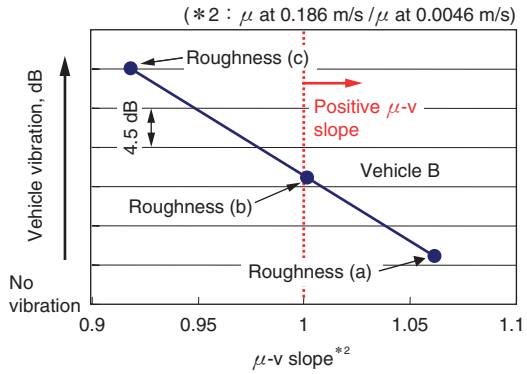

Fig. 14 Relationship between vehicle vibration amount and μ-v slope (Results of actual unit testing: For roughness (a), (b), (c))

3. 2. Coating Technology for Friction Surfaces of Planetary Gears

As stated above, the planetary gear top land in a planetary gear type torque-sensing LSD requires a moderate concave-convex shape on the surface to secure anti-vibration performance, but this shape increases wear due to increased local surface pressure at the friction surface. This pressure quickly wears out the concave-convex pattern, and reduces durability. In other words, there is a trade-off relationship between anti-vibration performance (concave-convex shape) and durability (wear and seizure) as shown in **Fig. 15**. This trade-off can be resolved by applying a carbon-based hard-coating using the magnetron sputtering technique, which is a kind of advanced physical vapor deposition (PVD) method. One example is the a-C:H:W nano multilayer coating consisting of tungsten carbide (WC) and diamond-like carbon (DLC) [7]. A carbon-based hard-coating can be applied to maintain an optimal concave-convex shape that has been designed for the sliding planetary gear circumference at a micron level. **Figure 16** shows an SEM image of a fracture surface on a planetary gear top land that was formed with roughness profile (a) and coated using a carbon-based hard-coating. **Figure 16** shows that from the substrate there is a coating of Cr, WC and WC/DLC multilayer coating approximately 3 μm thick in total. Furthermore, in the uppermost coating it can be seen that roughness is in parallel with sliding direction. This coating contributes to improving the seizure resistance of the planetary gear type torque-sensing LSD.

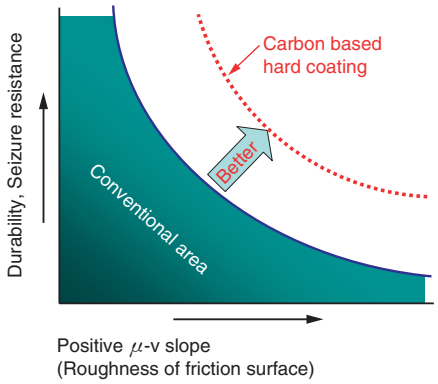

Fig. 15 Relationship between durability and μ-v slope

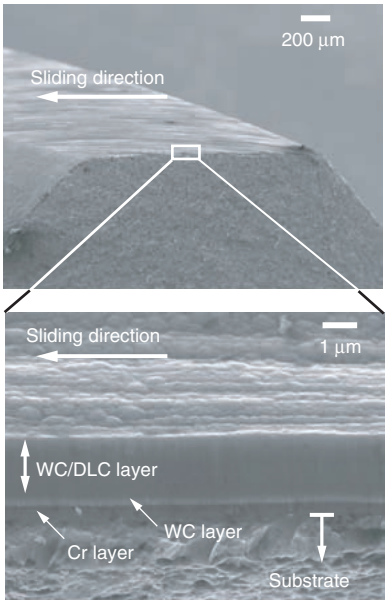

Fig. 16 SEM image of planetary gear fracture cross-section with carbon-based hard-coating

Figure 17 shows a schematic illustration of a Falex friction tester, which was used to study how to improve the seizure limit. The friction coefficients of two types of pins (with and without the carbon-based hard-coating) were measured by placing each pin between V blocks with an angular aperture of 96 degrees and rotating the pin. The tightening load applied on the V blocks was gradually increased and the load at which the friction coefficient rapidly increased was determined as the seizure limit. **Figure 18** shows that seizure resistance was significantly higher for the pin with the carbon-based hard-coating than the pin without. This showed that the trade-off issue of seizure resistance caused by the concave-convex shape could be resolved by carbon-based hard-coating technology, so that the contradiction between the μ-v characteristic (anti-vibration performance) and wear/seizure properties could be resolved as shown in **Fig. 15**.

Next, the effect of the surface pressure increase caused by the concave-convex shape was studied. As **Fig. 19** shows, the contact surface pressure was decreased by changing the line-contact V blocks with internal surface-contact R blocks that have a curvature radius of 4.15 mm. The contact area (more specifically, the surface pressure) was changed by using two types of pin specimens with different outer diameters (radius: 4 mm and 3.175 mm). The surface roughness was set to *Ra*=0.55 μm on the block side, and *Ra*=2 μm on the pin side. **Figure 20** shows the effect of surface pressure, or contact area, on the μ-v characteristic.

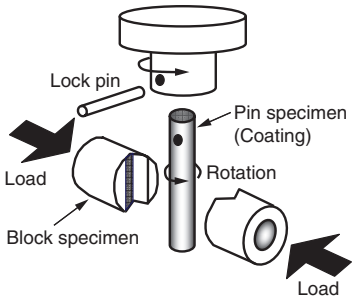

Fig. 17 Schematic diagram of a Falex friction tester

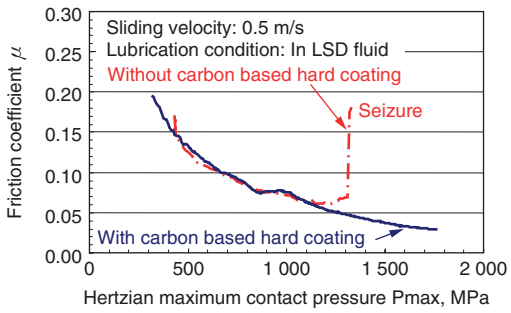

Fig. 18 Critical load test for seizure using a Falex friction tester

According to **Fig. 20**, in the case of a smaller pin outer diameter, or higher surface pressure, (**Fig. 19**(b), 912 MPa), the μ-v slope becomes negative. In contrast, in the case of a larger pin outer diameter, or lower surface pressure, (**Fig. 19**(a), 319 MPa), the μ-v slope becomes positive. In this case, the lower surface pressure is moderate.

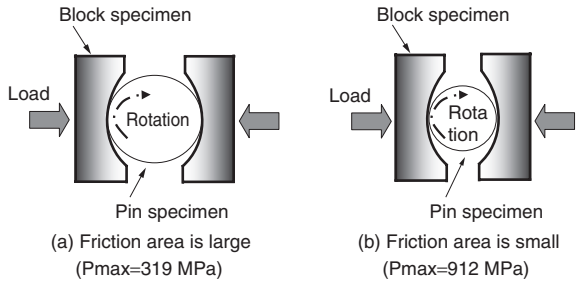

Fig. 19 2 test pieces of differing surface pressures and sliding surface area

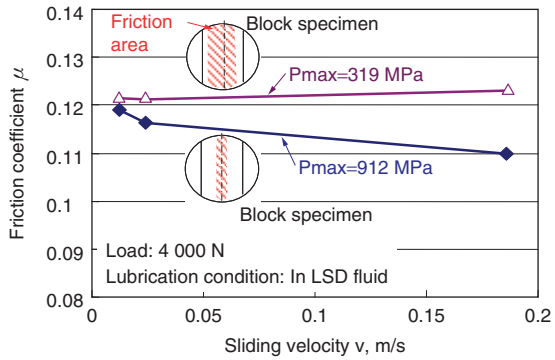

Fig. 20 Effects of surface pressure and sliding surface area on μ-v characteristics measured using a Falex friction tester

These results are also shown in **Fig. 21** as the relationship between the μ-v slope and the contact pressure on a friction surface with profile (a). As described above, friction surfaces require this concave-convex shape to obtain a positive μ-v slope.

Meanwhile, if a friction surface is given a concave-convex shape, its surface pressure will increase, and as described above, excessive surface pressure will induce a negative μ-v slope.

This is assumed to be caused by wear or separation generated by the excess surface pressure, which disrupts the formation of films such as the extreme pressure reaction film formed by the extreme pressure additives in the fluid, and the organic adsorbed film formed by the friction modifier (FM). Therefore, it is possible to secure a positive μ-v slope even if this planetary gear type torque-sensing LSD is given a concave-convex shape as long as the surface pressure is kept below the (d) point.

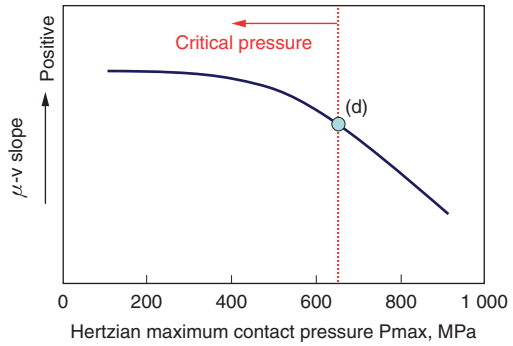

Fig. 21 Relationship between μ-v slope and contact surface pressure

Based on these results, it is possible to achieve stable friction characteristics by securing an appropriate sliding area on the planetary gear top lands and the housing bore surfaces.

As described above, even if the planetary gear type torque-sensing LSD shown in **Fig. 22** is used on gear portions where the sliding environment is severe, its reliability is assured using advanced tribological technology. This research and development focusing on tribology has improved the reliability and quietness of the planetary gear type torque-sensing LSD.

This planetary gear type torque-sensing LSD is used widely by Japanese and overseas vehicle manufacturers under the product name Torsen Type C®.

Fig. 22 Appearance of developed planetary gear type torque-sensing LSD (Vehicle B type)

4. Summary

(1) Anti-vibration performance was improved by providing the appropriate roughness on the planetary gear circumference to create a positive μ-v slope as a vibration control technology for a planetary gear type torque-sensing LSD.

(2) The effect of roughness on the μ-v characteristic of an actual unit was identified qualitatively based on mixed lubrication analyses that modeled the roughness of the planetary gear circumference and housing bore surface.

(3) Wear resistance and seizure resistance, which have a trade-off relationship with the surface concave-convex shape, were secured by applying a carbon-based hard-coating on the planetary gears and optimizing the friction area.

(4) Providing the concave-convex shape and applying the carbon-based hard-coating to the planetary gear circumference significantly improved the reliability and quietness of the planetary gear type torque-sensing LSD.

References

1) Y. Yamashita: The Synergy Study with the Torque Sensing Type Limited Slip Differential (LSD) and Vehicle Dynamics Control System of 4WD Vehicle, JSAE Proceedings, No. 90-02 (2002) 5.
2) N. Sakai: Technology Movement of Torsen Differential for All-Wheel-Drive vehicles (AWD), The Tribology, No. 230 (2006) 28.
3) Y. Yamamoto and M. Kaneta: Tribology, Rikogakusha Publishing (1998) 46.
4) M. Tohyama, T. Ohmori, S. Sanda, F. Ueda: Anti-Shudder Mechanism of ATF Additives (Part 1), Journal of Japanese Society of Tribologists, Vol. 47, No. 7 (2002) 49.
5) M. Tohyama, T. Ohmori, S. Sanda, F. Ueda: Anti-Shudder Mechanism of ATF Additives (Part 2), Journal of Japanese Society of Tribologists, Vol. 47, No. 7 (2002) 59.
6) T. Murakami, T. Hara, J. Ando: Clutch Friction Characteristic Optimized by Micro-Surface Shape, Toyoda Koki Technical Review, Vol. 44, No. 1 (2003) 9.
7) T. Kanamori: Application Example of DLC (Engine parts), Handbook of Diamond-Like Carbon Films, NTS (2006) 142.


J. ANDO*


H. ANDO**


H. SAITO***


H. TAKUNO**


T. HARA**


N. SAKAI****


Y. YAMASHITA*****


M. TOHYAMA******


T. OHMORI*****

* *Driveline System Engineering Dept., Bearing & Driveline Operations Headquarters, Doctor of Engineering*
** *Driveline System Engineering Dept., Bearing & Driveline Operations Headquarters*
*** *Experiment & Analysis Dept., Bearing & Driveline Operations Headquarters*
**** *Advanced Fundamental Research Dept., Research & Development Center, Research & Development Headquarters*
***** *Development Dept., Toyoda-koki Automotive Torsen Co.*
****** *Tribology Lab., Mechanical System Research Div., Toyota Central R&D Labs., Inc., Doctor of Engineering*
******* *Mechanical System Research Div., Toyota Central R&D Labs., Inc., Doctor of Engineering*